

The Jackson Laboratory

The Mouseion at the JAXlibrary

Faculty Research 2023

Faculty & Staff Research

6-1-2023

Simultaneous evaluation of treatment efficacy and toxicity for bispecific T-cell engager therapeutics in a humanized mouse model.

Jiwon Yang

Jing Jiao

Kyle Draheim

Guoxiang Yang

Hongyuan Yang

See next page for additional authors



Follow this and additional works at: <https://mouseion.jax.org/stfb2023>

Authors

Jiwon Yang, Jing Jiao, Kyle Draheim, Guoxiang Yang, Hongyuan Yang, Li-Chin Yao, Leonard D. Shultz, Dale L Greiner, Deepa Rajagopal, Sandrine Vessillier, Curtis C Maier, Sunish Mohanan, Danying Cai, Mingshan Cheng, Michael A Brehm, and James G. Keck

RESEARCH ARTICLE

Simultaneous evaluation of treatment efficacy and toxicity for bispecific T-cell engager therapeutics in a humanized mouse model

Jiwon Yang¹  | Jing Jiao¹ | Kyle M. Draheim¹ | Guoxiang Yang¹ | Hongyuan Yang¹ | Li-Chin Yao¹ | Leonard D. Shultz² | Dale L. Greiner³ | Deepa Rajagopal⁴ | Sandrine Vessillier⁴ | Curtis C. Maier⁵ | Sunish Mohanan⁶ | Danying Cai¹ | Mingshan Cheng¹ | Michael A. Brehm³  | James G. Keck¹

¹The Jackson Laboratory, Sacramento, California, USA

²The Jackson Laboratory, Bar Harbor, Massachusetts, USA

³Program in Molecular Medicine, Diabetes Center of Excellence, University of Massachusetts Chan Medical School, Worcester, Massachusetts, USA

⁴Biotherapeutics Division, National Institute for Biological Standards and Control, Hertfordshire, UK

⁵Non Clinical Safety, GlaxoSmithKline plc, Collegeville, Pennsylvania, USA

⁶NonClinical Safety and Pathobiology, Gilead Sciences Inc', Foster City, California, USA

Correspondence

Michael A. Brehm, Program in Molecular Medicine, Diabetes Center of Excellence, University of Massachusetts Chan Medical School, Worcester, MA 01605, USA.

Email: michael.brehm@umassmed.edu

James G. Keck, The Jackson Laboratory, 1650 Santa Ana Avenue, Sacramento, CA 95838, USA.

Email: james.keck@jax.org

Funding information

HHS | NIH | National Cancer Institute (NCI), Grant/Award Number: CA034196; HHS | NIH | National Institute of Allergy and Infectious Diseases (NIAID), Grant/Award Number: AI132963; HHS | NIH | NIDDK | Division of Diabetes, Endocrinology, and Metabolic Diseases (DEM), Grant/Award Number:

Abstract

Immuno-oncology (IO)-based therapies such as checkpoint inhibitors, bi-specific antibodies, and CAR-T-cell therapies have shown significant success in the treatment of several cancer indications. However, these therapies can result in the development of severe adverse events, including cytokine release syndrome (CRS). Currently, there is a paucity of in vivo models that can evaluate dose-response relationships for both tumor control and CRS-related safety issues. We tested an in vivo PBMC humanized mouse model to assess both treatment efficacy against specific tumors and the concurrent cytokine release profiles for individual human donors after treatment with a CD19xCD3 bispecific T-cell engager (BiTE). Using this model, we evaluated tumor burden, T-cell activation, and cytokine release in response to bispecific T-cell-engaging antibody in humanized mice generated with different PBMC donors. The results show that PBMC engrafted NOD-*scid* *Il2rg*^{null} mice lacking expression of mouse MHC class I and II (NSG-MHC-DKO mice) and implanted with a tumor xenograft predict both efficacy for tumor

Abbreviations: ADCC, antibody-dependent cellular cytotoxicity; B-ALL, B-cell precursor acute lymphoblastic leukemia; BiTE, bispecific T-cell engager; CRS, cytokine release syndrome; GVHD, graft-versus-host disease; IL, interleukin; IL2rg, IL-2 receptor subunit γ ; IO, Immuno-oncology; IR, Irradiated; mAb, monoclonal antibody; MHC, major histocompatibility complex; MHC-DKO, NSG-*H2-Ab1*^{em1mw} *H-2K*^{tm1Bpe} *H-2D*^{tm1Bpe}; NOD, NOD/ShiLtJ; NSG, NOD-*scid* *Il2rg*^{null}; PBL, peripheral blood lymphocyte; PBMC, peripheral blood mononuclear cell; PD-1, programmed death-1; scFv, single-chain variable fragments; scid, severe combined immunodeficiency; TNF, tumor necrosis factor.

This is an open access article under the terms of the [Creative Commons Attribution](https://creativecommons.org/licenses/by/4.0/) License, which permits use, distribution and reproduction in any medium, provided the original work is properly cited.

© 2023 The Authors. *The FASEB Journal* published by Wiley Periodicals LLC on behalf of Federation of American Societies for Experimental Biology.

DK104218; HHS | NIH | NIH Office of the Director (OD), Grant/Award Number: OD026440; UK Department of Health's Policy Research Programme, Grant/Award Number: 044/0069

control by CD19xCD3 BiTE and stimulated cytokine release. Moreover, our findings indicate that this PBMC-engrafted model captures variability among donors for tumor control and cytokine release following treatment. Tumor control and cytokine release were reproducible for the same PBMC donor in separate experiments. The PBMC humanized mouse model described here is a sensitive and reproducible platform that identifies specific patient/cancer/therapy combinations for treatment efficacy and development of complications.

KEYWORDS

cytokine release syndrome, humanized mouse, immune toxicity, therapeutic, cytokine storm

1 | INTRODUCTION

Immuno-oncology (IO)-based therapies are an evolving powerful treatment strategy that targets the immune system and harness it to directly kill tumor cells.^{1,2} There are numerous approaches for immuno-oncology therapeutics which include cell-based therapies (CAR-T), immune-checkpoint inhibitors (anti-PD-1, anti-CTLA), antibody-based therapies (T-cell engagers and ADCC), and cytokine therapies.^{3,4} As these therapies directly target the patient's immune system, they have the potential for broad activity across multiple types of cancer.⁵ Several studies have shown that T cells are major effector cells in anti-tumor immunity.^{6,7} A bispecific T-cell engager (BiTE) enhances the anti-tumor capabilities of T cells by re-directing them to recognize tumor-specific antigens. Most BiTEs have a flexible linker that connects two single-chain variable fragments (scFv), with one scFv binding to CD3 on T cells and the second scFv binding to a tumor-specific antigen, resulting in antigen-specific but MHC-independent T-cell killing of tumor cells.⁸⁻¹¹ Several BiTEs are in clinical development for hematological cancers, and BiTEs targeting solid tumors are entering clinical trials as well.¹²

Currently, blinatumomab is the only FDA-approved BiTE for cancer therapy. Blinatumomab is a CD19xCD3 BiTE antibody approved for use in relapsed and/or refractory B-cell precursor acute lymphoblastic leukemia (B-ALL) as well as the treatment of minimal residual disease in patients with B-ALL in complete remission.¹³ Across multiple phase II trials, the rates of complete response following blinatumomab treatment range from 30% to 69%.¹⁴ Blinatumomab also prolongs survival in patients with relapsed/refractory (R/R) B-precursor acute lymphoblastic lymphoma (ALL) and for both Philadelphia positive and negative ALL.^{13,15-19} Based on these phase II trial data, the FDA granted accelerated approval to blinatumomab for the treatment of R/R B-ALL.

All oncology treatment modalities targeting immune cells, including IO therapies such as blinatumomab or other BiTEs, have the potential to induce severe toxicities. A common toxicity associated with several IO therapies is cytokine release syndrome (CRS).²⁰ Extensive immune cell engagement, proliferation, and activation lead to the rapid production of cytokines, which has patient-specific clinical impacts. For example, some patients develop CRS with higher cytokine responses while other patients only release very low level of cytokines, and the underlying mechanisms are not well understood.^{13,15,21} Many patients only have mild flu-like symptoms, myalgias, and/or a self-limiting fever. However, some patients experience a severe inflammatory syndrome including vascular leakage, hypotension, pulmonary edema, multi-system organ failure, and even death.²¹⁻²³ Since 2006, a variety of cytokine release platforms have been developed to identify potential for unanticipated CRS by mAbs prior to clinical trials.²⁴⁻²⁶ However, these in vitro platforms may not be able to differentiate adverse cytokine release by immunomodulatory therapeutics for cancer for which some level of cytokine release is expected. More complex in vitro systems which include cancer cells need to be developed to assess both efficacy and safety of IO therapies. A significant challenge for pre-clinical evaluation of BiTEs for toxicity and efficacy is the inherent differences among patient's immune systems. Clinical studies have shown that the severity of CRS does not necessarily correlate with the extent of cytokine release or the response to therapy.²⁷ Collectively, the variability between patients and the lack of clear correlations between treatment efficacy, cytokine level and CRS, makes the prediction of an individual's response to many drug treatments nearly impossible using tools currently available.

Mice are one of the most widely used animal models for the study of IO and for the validation and pre-clinical evaluation of IO therapies.²⁸ The four major mouse models used to assess immunotherapies include

(1) syngeneic mouse tumor models with fully immune-competent hosts, (2) genetically engineered mouse models, (3) chemically induced models, and (4) humanized mouse models. While the first three approaches are widely used, one major drawback is that they rely on the murine immune system, which does not recapitulate many aspects of the human immune response.^{29,30} Therefore, preclinical models recapitulating a functional human immune system are critically needed. Previous studies have demonstrated the potential of using humanized mouse models as a translational bridge for the study and prediction of CRS in vivo.^{24,27,31–34} In this paper, we describe the novel application of a humanized mouse model that can simultaneously evaluate both the efficacy of BiTEs to control tumor burden and the development of CRS and that captures variability in responses for individual patients.

2 | MATERIALS AND METHODS

2.1 | Human PBMC donors

Human PBMC recovered from leukopaks purchased from either Lonza (Basel, Switzerland) or StemCell Technologies (Vancouver, British Columbia) using a previously published protocol.³⁵ PBMCs were cryopreserved and thawed for injections into recipient mice. Commercial sources of donor PBMC are shown in Table 1.

2.2 | Cell lines

The Raji_Luc cell line is a clonal line that expresses Firefly luciferase (emission peak wavelength of 550 nm) and was obtained from Creative Biogene and cultured in RPMI1640 supplemented with L-glutamine, 10% fetal bovine serum (FBS), and 10 µg/mL Blasticidin S HCL.

TABLE 1 Human PBMC donor information.

Donor ID	Source
8485	Lonza
8130	Lonza
8259	Lonza
0471	Stem Cell Technologies
0523	Stem Cell Technologies
9602	Lonza
9636	Lonza
9664	Lonza

2.3 | Test articles

The amino acid sequences of blinatumomab CD19XCD3 have been previously patented. Anti-CD19-Fc knob and anti-CD3-Fc hole-encoding fragments were assembled by PCR, cloned into mammalian cell expression vector, and transiently transfected into HEK 293 cells (ATCC). Supernatants were collected, followed by immobilized metal affinity chromatography. The purity of the BiTE was confirmed by SDS/PAGE followed by Coomassie blue staining, and their concentration was determined by measuring the absorbance at 280 nm. The CD19xCD3 used for this paper has a 94.1% purity. Rituximab was purchased from Genentech, South San Francisco, CA, OKT3 from BioXCell, Lebanon, NH, and anti-CD28 from Ancell, Bayport, MN.

2.4 | Mice and health status

Female NSG-*H2-Ab1^{em1mvw}* *H-2K1^{tm1Bpe}* *H-2D1^{tm1Bpe}* mice (NSG-MHC-DKO, stock number 025216) were obtained from The Jackson Laboratory (Bar Harbor, ME) at 4–6 weeks of age. Following drug treatment, mice were observed daily for overall health including general appearance of the fur, mobility, and body weight. The animals were euthanized before they exhibited clinical signs and symptoms to avoid unnecessary pain and discomfort, according to standard ethical animal guidelines. All animal procedures were done in accordance with the guidelines of the Animal Care and Use Committee of The Jackson Laboratory and The University of Massachusetts Medical School and conformed to the recommendations in the *Guide for the Care and Use of Laboratory Animals* (Institute of Laboratory Animal Resources, National Research Council, National Academy of Sciences, 1996).

2.5 | Generation of humanized PBMC mice for the drug treatment

NSG-MHC-DKO mice were preconditioned with irradiation (100 cGy, IR) at least 4 h before human PBMC intravenous (IV) injection (10×10^6 or 15×10^6 per mouse). Five days after PBMC engraftment, these PBMC humanized mice received 2×10^6 Raji-Luc cells. Six days after PBMC engraftment, PBMC-NSG-MHC-DKO mice were injected intravenously (IV) with different drug treatments, including CD19XCD3 BiTE, Rituximab, OKT3, anti-CD28, or TGN1412. PBS injection was used as a negative control in all experiments.

2.6 | Flow cytometry

Spleen samples were processed into single-cell suspensions using the GentleMACS tissue dissociator (Miltenyi Biotec). The cells were passed through a 100- μ m screen and centrifuged. Whole blood (collected in heparin) or spleen cell suspension was stained with the indicated antibodies. The stained samples were resuspended in 125 μ L of 1X DPBS CMF for acquisition on the flow cytometer. Flow cytometric data acquisition was performed using the FACSCanto™ or FACSCantoII™ flow cytometer. Data were acquired using BD FACSDiva™ software (version 8.0 or higher). Antibodies and reagents used here included: BioLegend human CD45 BV510 clone HI30, mouse CD45 V421 clone 30-F11, CD19 APC clone HIB19, CD56 PE clone HCD56, CD14 APCCy7 clone M5E2, CD33 PECy7 clone P67.6, CD3 FITC clone UCHT1, CD4 PECy7 clone SK3, CD8 APC clone SK1, CD69 BV510 clone FN50, and 7AAD.

2.7 | In vivo bioluminescence imaging

Tumor progression of Raji-Luc was monitored by BLI (bioluminescence imaging) using a Xenogen IVIS LUMINA III in vivo Imaging System (PerkinElmer). For bioluminescence in vivo imaging, mice with Raji-Luc engraftment were anesthetized with isoflurane, injected i.p. with D-luciferin (150 mg/kg), and placed into the imaging chamber of an IVIS imaging system. For bioluminescence quantification, a region of interest (ROI) was drawn manually and bioluminescence was recorded as radiance (peak photon/s/cm²/sr). Levels of bioluminescence for mAb or BiTE-treated mice were normalized to levels in PBS-treated mice.

2.8 | Cytokine analysis

Mice were bled at the indicated time points and serum was collected and analyzed for human cytokines (IFN- γ , IL10, IL6, IL2, IL4, and TNF α) using a BD Cytometric Bead Array (CBA) Human Th1/Th2 Cytokine kit II (BD-Biosciences). Cytokine levels were shown as either pg/mL detected or as a fold increase normalized to the PBS-treated mice for each unique donor.

2.9 | Statistical analysis

Statistical analyses were performed using a parametric Student's *t*-test (GraphPad Prism software V6.0) and as indicated in each figure legend. A two-way ANOVA test was

performed for multiple comparisons (GraphPad Prism software V6.0). * $p \leq .05$, ** $p \leq .01$, *** $p \leq .001$, **** $p \leq .0001$. Analysis of tumor size and cytokine values by concentration was carried out using multivariate regression within each donor. Concentration was used as a categorical value so no assumption of patterns by concentration was assumed. Fold changes from baseline control (PBS) were examined for tumor size. Both fold changes and log₁₀ values of cytokines were estimated by concentration. Differences in patterns of tumor size and cytokine values between donors were estimated using an interaction term (concentration and donor) in the regression model and the interaction was tested using a likelihood ratio test. Unadjusted *p*-values are shown for the interaction terms. A very conservative Bonferroni correction would use $p < .00083$ for statistical significance (controls the α -level for at least one false discovery). Error bars on the graphs are 95% confidence intervals.

3 | RESULTS

3.1 | Toxicity and efficacy of CD19xCD3 BiTE in PBMC-humanized mice

In the clinic, a transient cytokine elevation is detected following the first dose of blinatumomab while subsequent doses provoke minimal cytokine release.³⁶ We tested the impact of blinatumomab analog CD19xCD3 treatment in PBMC-engrafted NSG-MHC-DKO mice on the levels of engrafted human immune cells and on cytokine release (Figure 1A). NSG-MHC-DKO mice do not develop the acute xeno-GVHD that is observed in NSG mice after engraftment of PBMC and are an effective model to study human T-cell activation in the absence of direct responses to xenogeneic murine MHC.³⁷ NSG-MHC-DKO mice were irradiated (100 cGy) and injected with PBMC (15×10^6) by IV injection. Six and 8 days post-PBMC injection, mice were IV treated with PBS, OKT3 anti-CD3 mAb (0.25 mg/kg), or CD19xCD3 bispecific antibody (0.1 mg/kg). Whole blood was collected 6 h after treatment on day 6 and 6 h after treatment on day 8, to determine if cytokine production would be minimal after the second dose as described in the clinic with blinatumomab.³⁶ Blood was also collected on day 8 prior to the second treatment for flow cytometry and human cytokine analysis (Figure 1A). Human CD3 T cell levels, including both CD4+ and CD8+, were significantly decreased after the first and second treatment with OKT3 but not after CD19xCD3 bispecific antibody treatment (Figure 1B). This decrease in the levels of human T cells also correlated with the significant decrease in total human CD45+ cell levels, as the majority of human cells at this time point are CD3+. Significant levels of cytokines,

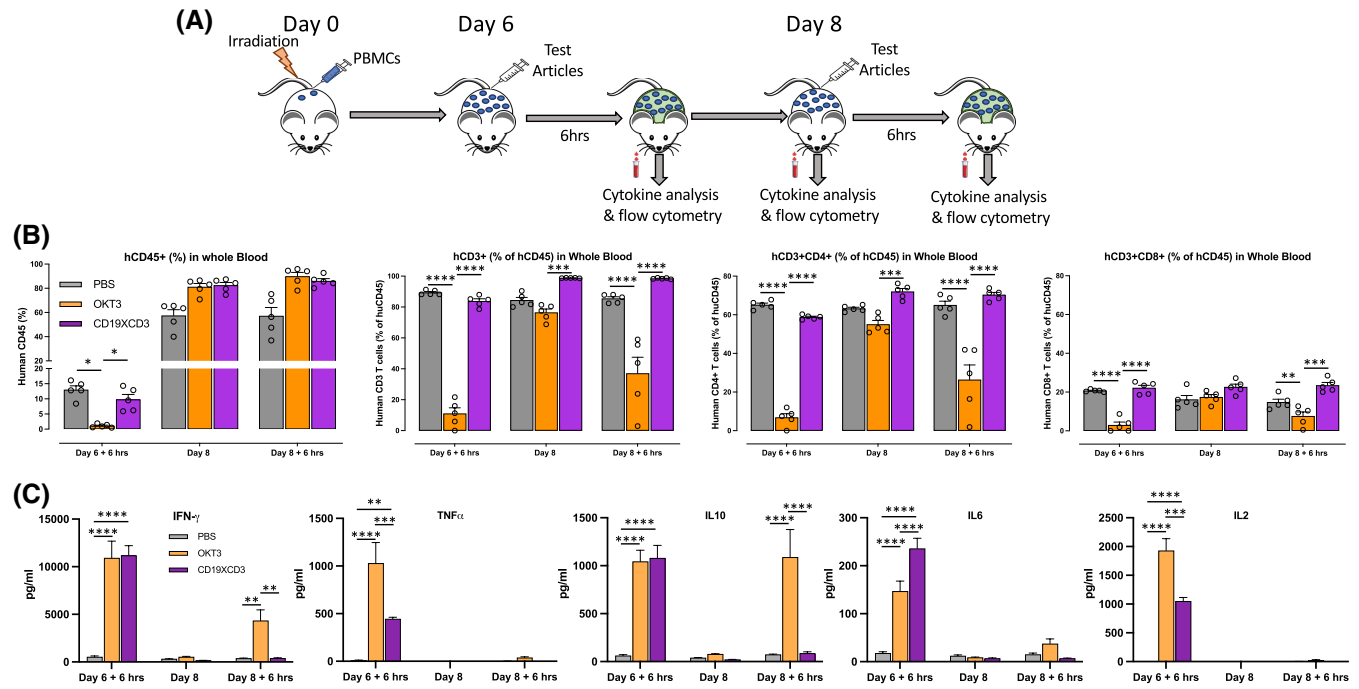


FIGURE 1 Human immune cell populations and cytokine release with various IO treatments in humanized NSG-MHC-DKO mice. (A) NSG-MHC-DKO female mice were irradiated (100 cGy) and injected with PBMC (15×10^6) via the tail vein. Six and 8 days post-PBMC injection, mice were IV injected with PBS, OKT3 (0.25 mg/kg), or CD19xCD3 bispecific antibody (0.1 mg/kg). Whole blood was collected 6 h after treatment on day 6 and on day 8 and on day 8 prior to the second treatment for flow cytometry and human cytokine analysis. (B) Blood samples were stained with antibodies specific for human CD45, CD3, CD4, and CD8. Symbols indicate individual mice and averages are shown by the bars. (C) Sera were collected and evaluated for levels of human IFN- γ , IL10, IL6, TNF α , and IL2. The data are representative of three independent experiments. * $p < .05$, ** $p < .01$, *** $p < .001$, **** $p < .0001$.

including IFN γ , TNF α , IL10, IL6, and IL2, were detected after a single dose of either OKT3 or CD19xCD3 bispecific antibody (Figure 1C). The second dose of OKT3 induced relatively low amounts of other cytokines with the exception of IFN γ and IL10. The second dose of BiTE induced very low amounts of cytokine, as compared to the levels of IFN γ and IL10 stimulated by OKT3, mimicking cytokine release kinetics in patients.²⁸

We next used the PBMC-humanized NSG-MHC-DKO model to test in vivo efficacy of IO therapeutics (Figure 2A). NSG-MHC-DKO mice will support the growth of Raji-Luc cells (luciferase expressing Raji tumor cells) as shown in Figure S1 and this growth is measurable by bioluminescent imaging using an IVIS[®] Bioimaging System. NSG-MHC-DKO mice engrafted with PBMC show similar tumor burden to unengrafted mice at early time points, but tumor growth is reduced at later time points as shown with three different PBMC donors (0523, 9602, and 9636) in Figure S1. The reduced tumor burden is attributed to the alloantigen-specific T-cell response against the Raji-Luc cells. PBMC-humanized NSG-MHC-DKO were IV injected with Raji-Luc tumor cells (2×10^6 cells) on study day 5 (Figure 2A). Approximately 24h after the tumor cell injection (study day 6), mice were dosed with various

IO therapeutics. Human cytokine levels and tumor burdens were determined along with clinical observations and histology to gauge the effects of different IO therapies in humanized mice bearing human B lymphoblastoid cells (Raji-Luc cells that express CD19 and CD20 and are, therefore, targets for both CD19xCD3 BiTE and rituximab). To examine whether our PBMC-engrafted NSG-MHC-DKO platform can recapitulate patient-specific cytokine release, we tested NSG-MHC-DKO mice engrafted with three different PBMC donors (8485, 8130, and 8259) and injected with Raji-Luc cells prior to treatment with PBS, anti-CD28, Rituximab, CD19xCD3 BiTE, or a combination of Rituximab and CD19xCD3 BiTE. Rituximab was considered a well-established therapeutic for B-cell lymphomas and was used for comparison to CD19xCD3 BiTE treatment.³⁸ At day 5 after PBMC engraftment, mice were confirmed to have similar percentages of circulating hCD45+ cells by flow analysis (Donor 8485, 11.6 ± 0.7 ; Donor 8130, 14.2 ± 1.1 ; and Donor 8259, 16.4 ± 1.0). Upon CD19xCD3 (0.25 mg/kg) treatment, mice engrafted with individual PBMC samples showed different cytokine release profiles (Figure 2B). Mice engrafted with PBMC from donor 8485 and treated with CD19xCD3 showed significant levels of human IFN- γ , TNF α , IL10, IL6, IL4, and IL2

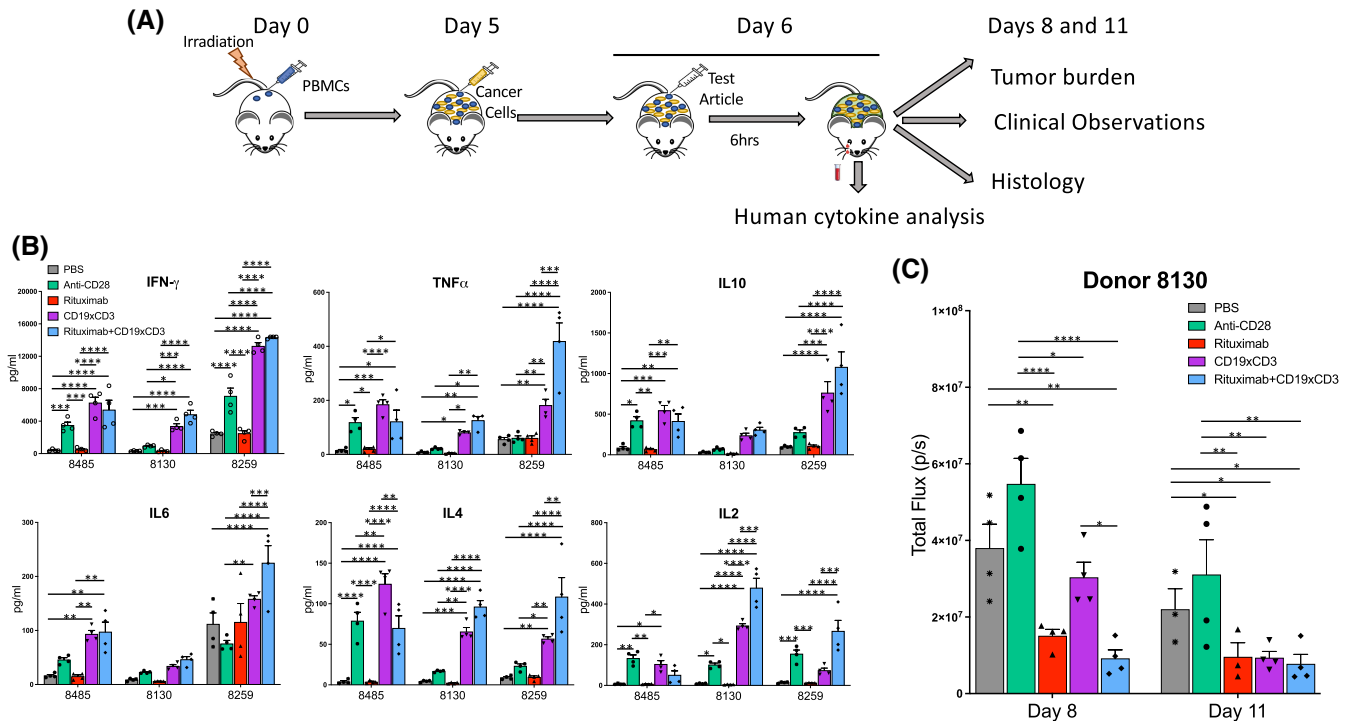


FIGURE 2 Cytokine release with various IO treatments in humanized NSG-variant mice bearing Raji-Luc tumor is donor dependent. (A) Cohorts of NSG-MHC-DKO female mice were irradiated (100cGy) and injected with PBMC (10 to 20×10^6 from either of three different donors: 8485, 8130, and 8259) via the tail vein. After the human immune cells had successfully engrafted (study day 5), 2×10^6 Raji-Luc cells were injected via the tail vein. Twenty-four h after the tumor cell injection (study day 6), mice were dosed with PBS, anti-CD28 (1 mg/kg), Rituximab (5 mg/kg), CD19xCD3 bispecific antibody (0.25 mg/kg), or a combination of Rituximab (5 mg/kg) and CD19xCD3 bispecific antibody (0.25 mg/kg) by IV injection. Human cytokine levels and tumor burden were measured to gauge the effect of various IO in humanized mice bearing human B lymphoblastoid cells. (B) Three PBMC donors were evaluated for cytokine release after various IO treatments. Sera were collected 6 h after the injection and analyzed for human IFN- γ , TNF α , IL10, IL6, IL4, and IL2. Each symbol represents an individual mouse. Mean cytokine levels (pg/mL) \pm SEM, $n = 5$ /group. (C) Humanized mice engrafted with PBMC from donor 8130 were imaged using an IVIS imaging system to determine tumor burden on study days 8 and 11 as described in Materials and Methods. * $p < .05$, ** $p < .01$, *** $p < .001$, **** $p < .0001$.

as compared to the PBS-treated control mice. Mice engrafted with PBMC from donor 8130 and treated with CD19xCD3 showed significant levels of human IFN- γ , TNF α , IL 4, and IL2 as compared to the PBS-treated control mice. Mice engrafted with PBMC from donor 8259 and treated with CD19xCD3 showed significant levels of human IFN- γ , TNF α , IL10, and IL4 as compared to the PBS-treated control mice. As previously described,³¹ treatment with anti-CD28 stimulated cytokine release in a donor-specific manner for human IFN- γ , TNF α , IL10, IL4, and IL2. Anti-CD28 treatment did not stimulate the release of human IL6 from any donors. Although Rituximab treatment alone did not stimulate significant cytokine release as compared to PBS-treated control mice, combination treatment with CD19xCD3 and Rituximab enhanced production of specific cytokines in a donor-specific manner (Figure 2B). In mice engrafted with PBMC from donor 8259, significantly higher levels of human TNF α , IL6, IL4, and IL2 were observed with combination compared to the respective single agent treatments. Donor 8130 humanized mice

showed significantly enhanced level of IL2 release after combination treatment with CD19xCD3 and Rituximab as compared to single agent treatments.

Tumor burden was monitored in NSG-MHC-DKO mice engrafted with PBMC from donor 8130 and Raji-Luc cells using the IVIS[®] Bioimaging System. Treatment with Rituximab and the combination of Rituximab and CD19xCD3 resulted in a significant reduction of tumor burden as compared to PBS and anti-CD28 treated mice (Figure 2C) on day 8, 2 days after injection of test articles (Figure 2A). By study day 11, the groups treated with Rituximab, CD19xCD3 alone, or as a combination, all showed a significant reduction in tumor burden as compared to PBS and anti-CD28 treated mice. The reduction in tumor burden between days 8 and 11 for the PBS-treated mice is attributed to the human T-cell engraftment in these mice, although this reduction was not statistically significant ($p = .2$). Tumor burdens for mice treated with anti-CD28 ($p = .009$) or treated with CD19xCD3 BiTE ($p = .02$) were significantly decreased from day 8 to day 11. These data suggest that PBMC-engrafted NSG-MHC-DKO

mice implanted with a xenograft tumor can determine both efficacy and cytokine release within the same experiment.

3.2 | Dose-response profiles from multiple donors in PBMC-humanized mice

Clinical data suggest that transient cytokine levels increased with higher doses of blinatumomab.³⁹ Next, we examined CD19xCD3 dose-response from NSG-MHC-DKO mice humanized with several different PBMC donors (Figure 3A). While there were similarities for some of the donors when looking at a single cytokine, each donor had a unique profile when taking six cytokines (IFN- γ , TNF α , IL10, IL6, IL4, and IL2) into account (Table S1). The analysis of interaction trends for individual cytokines among donors showed donor-specific patterns with significant differences between production of cytokines from each donor as shown in Table S1. Interestingly, while all the donors had comparable engraftment at the time of dosing (Donor 0471, 7.6 ± 0.9 ; Donor 0523, 13.06 ± 0.4 ; Donor 9602, 11.4 ± 0.9 ; Donor 9636, 14.4 ± 1.4 ; and Donor 9664, 16.2 ± 2.4), there was a broad spectrum of baseline levels for each of the cytokines evaluated. These differences impacted the evaluation of drug response when cytokine release was normalized to the PBS control group (Figure 3B). Serum cytokine levels for Donor 0471 post-CD19xCD3 treatment were all very high. However, when normalized for the high background, the BiTE-induced drug response for donor 0471 is minimal. Conversely, serum cytokine levels in mice humanized with Donor 9602 were relatively low, but the fold changes were higher than most of the other donors.

In vivo bioluminescence imaging at study days 8 and 10 (2 and 4 days after CD19xCD3 treatment) demonstrated donor-specific drug efficacy (Figure 3C,D). NSG-MHC-DKO mice engrafted with PBMC from donors 0471, 0523, and 9602 required a higher dose of CD19xCD3 BiTE to reach a statistical reduction in tumor burden. In contrast, mice engrafted with PBMC from donors 9636 or 9664 showed a significant reduction of tumor burden with lower doses of CD19xCD3 BiTE. The peak response day after the single treatment also varied among donors. Donors 0471 and 9664 demonstrated maximum efficacy 2 days post-treatment (day 8), while 9602 and 9636 maintained a significant reduction in tumor load for 4 days (day 10). These data demonstrate that the efficiency and kinetics for tumor control mediated by treatment with CD19xCD3 BiTE are donor dependent (Figure 3C,D). Representative IVIS images from mice engrafted with donor 9636 are shown in Figure 3E. Correlations between cytokine production and tumor control were also donor

specific (Figure 3 and Table S1). For example, mice engrafted with PBMC from donors 0471 and 0523 showed tumor control with only higher doses of BiTE treatment, and overall cytokine interactive trends (described in the Materials and Methods) were similar for these donors. However, PBMC from donor 9602 showed similar efficacy for tumor control as compared to donors 0471 and 0523, but the cytokine interactive trends from 9602 were significantly different. Mice engrafted with PBMC from donors 9636 and 9664 showed similar tumor control with lower doses of BiTE treatment, but cytokine interactive trends were significantly different. Mice engrafted with PBMC from donor 9636 showed the highest cytokine levels and the best tumor control. Collectively, these data demonstrate that immune cell responses to IO therapeutics are donor specific and that cytokine release profile or levels do not directly correlate with treatment efficacy.

3.3 | Platform reproducibility in PBMC-humanized mice

To evaluate the reproducibility of this platform, two cohorts of NSG-MHC-DKO mice were humanized with PBMC from donors 9636 and 9602 in two separate experiments and implanted with Raji-Luc cells 5 days after PBMC engraftment (Figure 2A). The PBMC used for each donor was collected from the same blood donated. On the sixth day after PBMC engraftment, mice were dosed with six different concentrations of CD19xCD3 BiTE. Serum concentrations of human cytokines were determined from samples taken 6 h after dosing and compared between the two cohorts. No significant differences were observed for human IFN- γ , TNF α , IL10, IL6, IL4, and IL2, between mice engrafted with the same donor PBMC (Figure 4A). Tumor burdens of Raji-Luc cells were monitored in the treated mice for several days after drug treatment using the IVIS[®] Bioimaging System. As was seen for cytokine release, the response of the various dosages of CD19xCD3 BiTE was not significantly different between mice engrafted with the same donor PBMC (Figure 4B). The data from two independent studies show that this platform is reproducible and reliable.

3.4 | Treatment-induced T-cell activation

To evaluate the impact of various CD19xCD3 doses on the subpopulations of engrafted human immune cells, whole blood and spleens from NSG-MHC-DKO mice engrafted with donor 8485 PBMC were collected 24 h after drug treatment and analyzed by flow cytometry. Treatment with anti-CD28 reduced the percentages of human CD45+

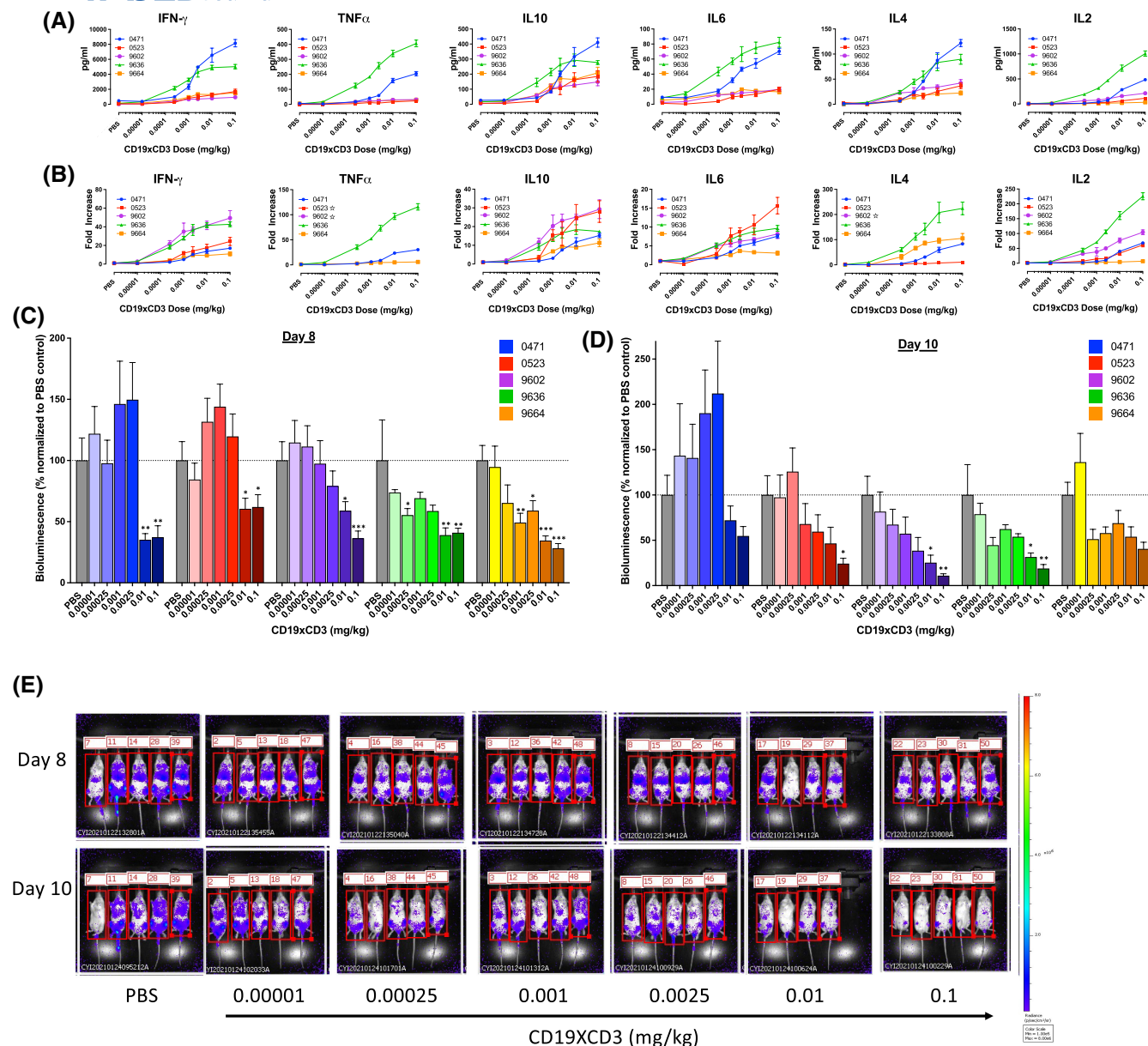


FIGURE 3 Cytokine release with CD19xCD3 bispecific antibody treatment is donor- and dose-dependent in humanized NSG-MHC-DKO mice bearing human B cell lymphoma. Irradiated NSG-MHC-DKO mice (100 cGy) were IV injected with 10×10^6 PBMC (study day 0) from five different donors, followed by IV injection of 2×10^6 Raji-Luc cells on study day 5. Six days post-PBMC injection, mice were IV treated with PBS or six concentrations of CD19xCD3 bispecific antibodies as indicated. Sera were collected 6 h after the injection for cytokine analysis and mice were imaged using an IVIS imaging system to determine tumor burden. (A, B) Sera samples were analyzed for human IFN- γ , TNF α , IL10, IL6, IL4, and IL2 levels and data are shown as either pg/mL (A) or fold change from PBS treatment (B) with $n = 4$ to 5 per group. TNF α and IL4 were below the limit of detection in the 9602 PBS group and in the 0523 PBS group and, therefore, fold changes were not calculated (indicated by the \star symbol in the graphs). (C, D) The efficacy profile of CD19xCD3 bispecific antibody at day 8 (C) and day 10 (D) in PBMC humanized NSG-MHC-DKO mice bearing Raji-Luc cells were measured using an IVIS imaging system. Data shown were normalized to the PBS control group. (E) Representative bioluminescence imaging data acquired by an IVIS imaging system that shows tumor burden on study days 8 and 10 of humanized mice engrafted with PBMC from donor 9636 ($n = 5$). $\ast p < .05$, $\ast\ast p < .01$, $\ast\ast\ast p < .001$.

cells and CD4 $^+$ T cells in blood and with no significant decrease in total cell numbers (Figure 5A). Mice treated with 0.1 and 0.001 mg/kg doses of CD19xCD3 BiTE showed significant decreases in the percentages of CD4 $^+$ T cells in blood, but these levels were increased in the spleen

(Figure 5A), suggesting that T cells were trafficking to the spleen after treatment. Treatment with the 0.001 mg/kg dose of CD19xCD3 BiTE resulted in higher numbers of CD4 T cells in the spleen. To examine T-cell activation status, CD4 and CD8 T cells were stained for CD69. Mice

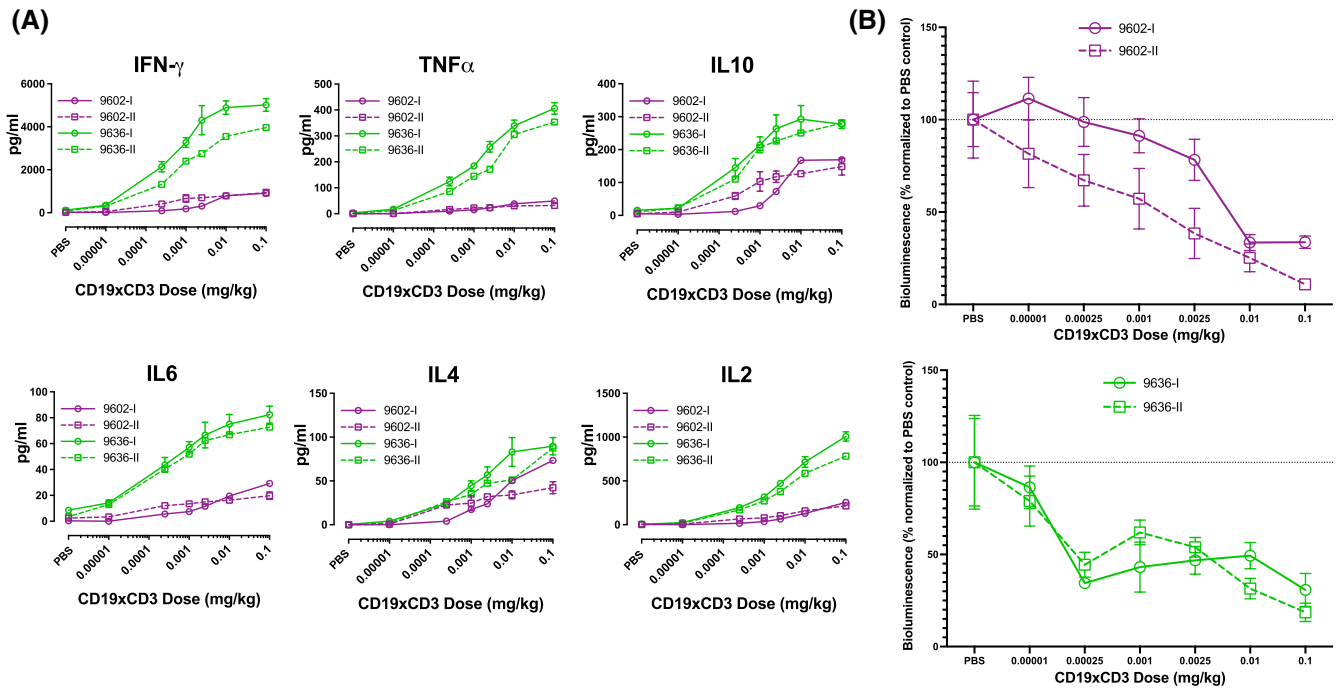


FIGURE 4 Cytokine release with CD19xCD3 bispecific antibody treatment is donor dependent and reproducible in humanized NSG-MHC-DKO mice bearing human B cell lymphoma. Irradiated NSG-MHC-DKO mice (100 cGy) were IV injected with 10×10^6 PBMC (study day 0) from donor 9602 or donor 9636 in two duplicate experiments (I and II). On study day 5, 2×10^6 Raji-Luc cells were IV injected. Six days post-PBMC injection, mice were IV treated with PBS, anti-CD28 (1 mg/kg), or six concentrations of CD19xCD3 bispecific antibodies as indicated. Sera were collected 6 h after the injection for cytokine analysis and mice were imaged using an IVIS imaging system to determine tumor burden. (A) The same PBMC donor (donor 9636 or donor 9602) was tested in two independent experiments to assess the reproducibility of our platform. Sera were analyzed for human IFN- γ , TNF α , IL10, IL6, IL4, and IL2 levels and data are shown as pg/mL. (B) The tumor burden was determined by bioluminescence imaging on study days 8 and 10 as described in Materials and Methods. The data from two independent studies show that the platform is reproducible and reliable. Data shown were normalized to the PBS control group.

treated with 0.1 and 0.001 mg/kg doses of CD19xCD3 BiTE showed significant increases in the percentages and numbers of CD69+ CD4 and CD8 T cells in the spleen but not the blood (Figure 5B). Representative flow cytometry staining is shown in Figure 5C.

PBMC-engrafted NSG-MHC-DKO mice have very low levels of engrafting human B cells, and this enables detection of CD19+ Raji cells by flow cytometry.³⁷ Flow cytometry analysis of the B-cell population (% of CD19⁺CD3⁻ Raji cells) in the mice indicated that 0.1 and 0.001 mg/kg doses of CD19xCD3 BiTE treatment significantly decreased the Raji cells in the blood and spleen (Figure 5D). However, the lowest dose (0.00001 mg/kg) of CD19xCD3 did not reduce Raji cell levels in blood and spleen, which correlated with the lower level of CD69 T-cell activation for this group (Figure 5B). In addition, the efficacy of CD19xCD3 treatment was dose dependent as mice treated with 0.1 mg/kg had significantly lower levels of CD19+/CD3- cells relative to mice treated with 0.001 mg/kg (0.58% and 10.5%, respectively, $p = .013$) (Figure 5D). It is important to note that human B cells from the injected PBMC do not survive in NSG models, and thus will not be targets for the CD19xCD3 BiTEs. Live animal imaging

of luciferase signal also supported this observation with the lowest concentration of CD19xCD3 0.00001 mg/kg showing similar Raji-Luc tumor burden compared to PBS control (Figure 5E). The anti-CD28 treatments did not significantly change tumor burden. The changes induced in T-cell activation phenotype with a single dose of CD19xCD3 BiTE were transient. T-cell populations (including total CD3+, CD3+/CD4+ and CD3/CD8+ and CD69+ CD4 and CD8 T cells) were comparable to the PBS control group 72 h after treatment (Figure S2). As shown with donor 9664, CD19xCD3 induced a transient cytokine release with peak level at 6 h, a decrease at 24 h, and return to basal levels by 72 h post-dosing (Figure S3). Levels of mouse CD45+ cells (percentages or total number) were not altered by treatment of PBMC-humanized NSG-MHC-DKO mice (Figure S4).

4 | DISCUSSION

BiTEs are a promising class of molecules in drug development, providing great potential for an off-the-shelf product for targeted immunotherapy.^{12,40} For example,

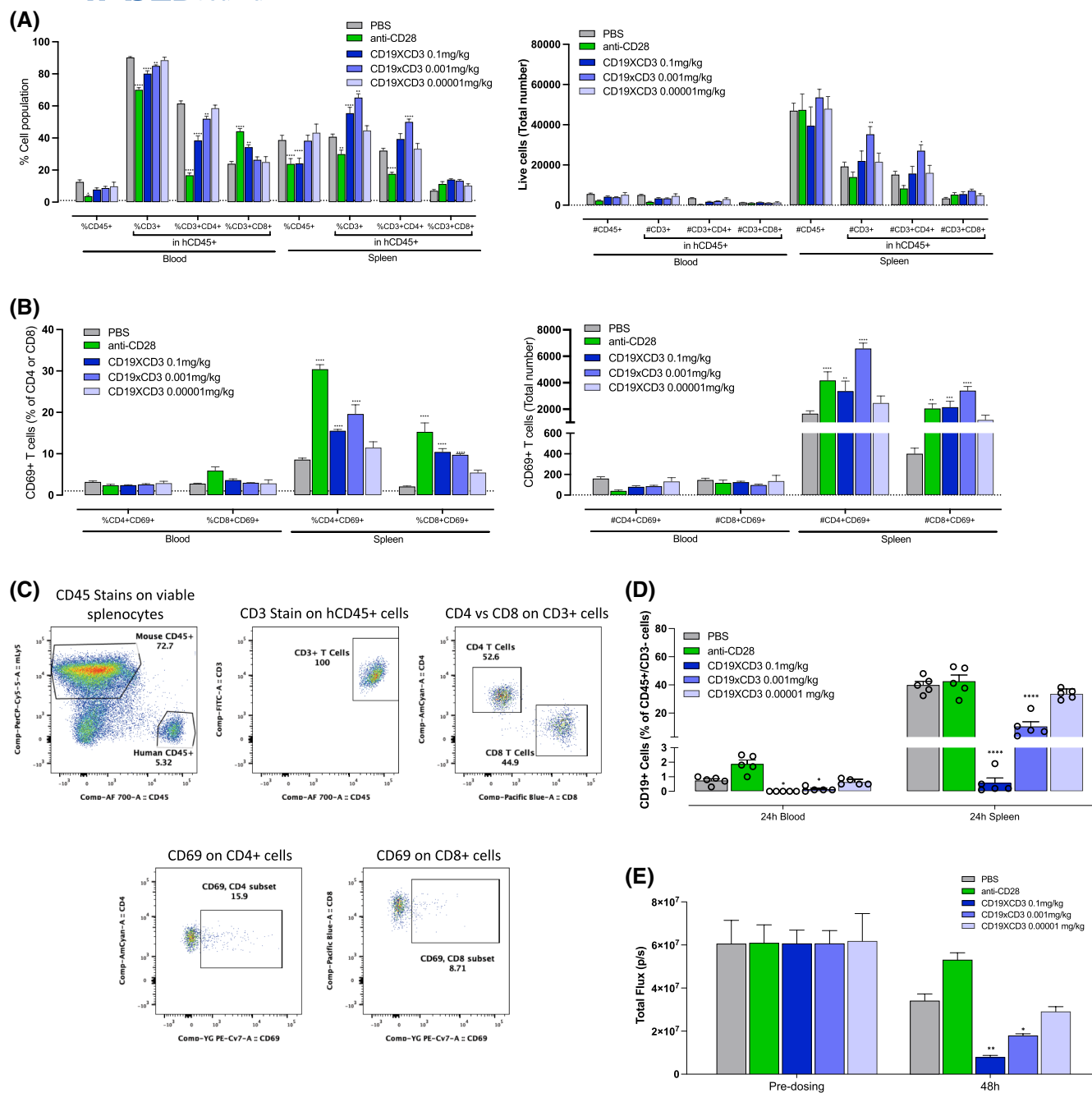


FIGURE 5 CD19xCD3 bispecific antibody treatment in humanized NSG-MHC-DKO mice bearing Raji-Luc tumor stimulates T-cell activation. NSG-MHC-DKO mice were irradiated (100cGy) and IV injected with 10×10^6 PBMCs (Donor 8485, study day 0), followed by IV injection of Raji-Luc cells (2×10^6) on study day 5. On study day 6, mice were IV treated with PBS, anti-CD28 (1 mg/kg), or three concentrations of CD19xCD3 bispecific antibodies, and whole blood and spleen were collected 24h after drug dosing. Blood and spleen single cells were prepared and stained for flow cytometry as described in the Materials and Methods. (A) Blood and spleen were evaluated for levels of human CD45+ cells, CD3+ T cells, CD4 T cells, and CD8 T cells, and (B) CD4 and C8 T cells were evaluated for expression of CD69. (C) Representative flow cytometry data are shown. (D) Treatment efficacy showing cell population (%CD19+ CD3- of CD45+) change from blood and spleen 24h post-dosing. (E) Humanized mice engrafted with PBMC from donor 8485 and Raji-Luc cells were imaged using an IVIS imaging system to determine tumor burden on study day 5 (pre-dosing) and day 8 (48h post-dosing) as described in Materials and Methods. The results are representative of three independent experiments. * $p < .05$, ** $p < .01$, *** $p < .001$, **** $p < .0001$.

blinatumomab showed clinical success in B-ALL with increased overall survival and reduction in the incidence of selected adverse events compared to standard of care

(SOC) chemotherapy. However, 7% of patients experienced a CRS event from the MT103-203 study.⁴¹ CRS and neurotoxicity are major challenges for the translation of

new BiTEs to effective therapies with reliable safety.²³ The mechanisms underlying the development of CRS are still poorly understood. Given the complexity of CRS, there is an urgent need for preclinical models, which can evaluate both BiTE efficacy and safety and predict the association between efficacy and immune-related toxicity. Here, we describe an established PBMC-humanized mouse model to evaluate CD19xCD3 BiTE, a blinatumomab analog, as a proof of principle for other new BiTE constructs. The results show that PBMC-engrafted NSG-MHC-DKO mice implanted with a tumor xenograft predict both cytokine release stimulated by CD19xCD3 BiTE and efficacy for tumor control. Moreover, our findings indicate that this PBMC-engrafted model also captures variability between donors for cytokine release and tumor control following treatment. Overall, this study demonstrates that the PBMC-engrafted NSG-MHC-DKO model can provide insights into the efficacy and safety of immunotherapies and can facilitate the selection of optimal starting doses in the clinic.

In response to CD19xCD3 BiTE, the PBMC-humanized mouse model reproduced several key features of human patient responses to blinatumomab. First, clinical studies suggested that IFN γ , IL6, and IL10 are detected at significant levels in the serum of patients treated with blinatumomab.³⁶ We also observed significantly increased serum levels of human IFN γ , IL6, IL10, TNF α , IL2, and IL4 at 6 h after treatment followed by a decrease at 24 h. A second dose of CD19xCD3 did not induce high levels of cytokine release, consistent with the clinical observations that only the first infusion causes CRS, and the subsequent infusions result in mild or reduced CRS.^{42,43} Secondly, our model captures the inherent variability in response between donors. Some donors show strong cytokine responses even with a low dosage, while other donors are less responsive to CD19xCD3 treatment and only respond to the higher BiTE doses. As reported, 5–15 $\mu\text{g}/\text{m}^2/\text{day}$ was used as the initial first dose of blinatumomab,³⁶ which is comparable to 0.001665 mg/kg to 0.004995 mpk dose in mice based on Conversion of Animal Doses to Human Equivalent Doses.⁴⁴ A dose of 60 $\mu\text{g}/\text{m}^2/\text{day}$ was established as the maximum tolerated dose of blinatumomab, which is comparable to a 0.01998 mg/kg dose in mice. The six doses we picked for blinatumomab analog CD19XCD3 study are within the range used for human patients. Dose curves performed on multiple donors suggest that each PBMC donor has a unique dose-response and cytokine release profile that is similar to the patient response to blinatumomab. Thirdly, blinatumomab can be used as a combination therapy with other drugs: e.g., TKI (Dasatinib) or PD-1 inhibitor pembrolizumab. In vitro studies also suggested that this combination therapy can provide benefit to some patients.⁴⁵ Results from

our humanized model (Figure 2C) suggest that combination treatment with CD19xCD3 BiTE and Rituximab may provide a beneficial effect in donor-specific manner. Moreover, our humanized model validated the overall effectiveness of Rituximab with limited CRS,⁴⁶ and enabled direct comparisons with the CD19xCD3 BiTE reagent for tumor burden and cytokine release.

Current clinical data suggest that increasing doses of BiTE can improve efficacy and that toxic cytokine release can be uncoupled from cytotoxic T-cell activity.⁴⁷ Therefore, ideal dose/exposure for BiTEs should increase cytotoxic T-cell activity but trigger relatively low cytokine release. At higher doses, BiTEs may lead to higher cytokine release from T cells and enhance activation of monocytes/macrophage, which in turn release more cytokines. Currently pre-treatment with corticosteroids along with dose escalation schemes are recommended to manage CRS.⁴⁸ Our humanized PBMC model provides a unique tool that may be useful to evaluate donor-specific therapeutic windows.⁴⁹ It was proposed that high tumor burden, aggressive disease condition, and abnormal macrophage activation are potential contributing factors to CRS.^{23,39} We used bioluminescent imaging data to show reduction in tumor burden as BiTE efficacy and systematic cytokine release as BiTE safety. Using our PBMC-humanized mouse platform (Figure 3), we were able to identify donors that showed treatment efficacy at low doses of CD19XCD3 (donor 9636) and donors that showed efficacy at only high doses (donor 0471). Moreover, we were able to determine the optimal treatment dose that showed efficacy but did not induce CRS in specific patient samples, and this varied for each donor tested. Finally, we also identified donors that may be a high risk for treatment, only showing efficacy with doses of CD19XCD3 that triggers strong CRS.

Human T cells are the predominant human immune cell population that survives in NSG mice and NSG-MHC-DKO mice engrafted with PBMC.^{37,50} Human B cells, myeloid cells, and NK cells are short lived in PBMC-engrafted NSG mice and NSG-MHC-DKO mice. Based on the high levels of human T cells in PBMC-engrafted NSG-MHC-DKO mice, the antibody-based therapeutics that induce significant cytokine release are T-cell engagers. For example, treatment with Rituximab in PBMC-engrafted NSG-MHC-DKO mice co-implanted with Raji tumors does not stimulate high levels of cytokines (Figure 3). Abnormal monocyte and macrophage activation are also an important source of systemic toxic cytokine release.^{39,47} Sublethal irradiation preconditioning of NSG-MHC-DKO mice will enable detectable CD14 human monocytes and CD56dim/CD16+ NK cell survival for 5–7 days at low levels in blood and spleen.³¹ Studies are ongoing to develop new humanized NSG mouse models that will enable enhanced survival of human myeloid and NK cells after

PBMC engraftment for safety and efficacy testing of antibody therapeutics.

The relationship between T-cell activation and drug efficacy was explored in this PBMC-humanized mouse model. For 9664 humanized mice, similar T-cell activation (%CD69+ CD8 of CD45) between dose 0.1 mg/kg and 0.001 mg/kg was detected 24 h post-dosing in the spleen; however, there is significant efficacy difference between these two different treatment doses, as shown in Figure 5E. In addition, anti-CD28 treatment induced higher T-cell activation but no efficacy indicating the importance of targeted therapy. Clinical data also suggest that nonresponding patients had similar levels of activated T cells as responders to blinatumomab monotherapy.⁴² Therefore, T-cell activation is not suitable to predict drug efficacy. Ongoing studies using this humanized PBMC model may determine a better biomarker to predict drug efficacy. Overall, these findings indicate that the PBMC-humanized mouse platform developed here is a sensitive and reliable approach to determine the optimal dose window for future patient treatment.

AUTHOR CONTRIBUTIONS

Jiwon Yang: Conceptualization, Investigation, Methodology, and Writing – Original Draft. **Jing Jiao:** Conceptualization, Investigation, and Methodology. **Kyle M. Draheim:** Conceptualization, Investigation, and Methodology. **Guoxiang Yang:** Conceptualization, Investigation, and Methodology. **Hongyuan Yang:** Conceptualization, Investigation, and Methodology. **Li-Chin Yao:** Conceptualization, Investigation, and Methodology. **Leonard D. Shultz:** Conceptualization and Writing – Original Draft. **Dale L. Greiner:** Conceptualization and Writing—Original Draft. **Deepa Rajagopal:** Investigation and Methodology. **Sandrine Vessillier:** Conceptualization, Investigation, Methodology, and Writing – Review and Editing. **Curtis C. Maier:** Writing – Original Draft and Writing – Review and Editing. **Sunish Mohanan:** Writing – Original Draft and Writing – Review and Editing. **Danying Cai:** Investigation and Methodology. **Mingshan Cheng:** Conceptualization, Investigation, and Methodology. **Michael A. Brehm:** Investigation, Writing – Original Draft, and Writing – Review and Editing. **James G. Keck:** Conceptualization, Investigation, Writing – Original Draft, and Writing – Review and Editing. All authors reviewed the article and approved the submitted version.

ACKNOWLEDGMENTS

The animal studies were reviewed and approved by the Animal Care and Use Committee of The Jackson Laboratory. The human biological samples were sourced

ethically and studies using human tissues were in accord with the terms of informed consent and reviewed and approved by the Institutional Review Board of The Jackson Laboratory. We thank George Reed at the UMass Chan Medical School for assistance with statistical analyses.

FUNDING INFORMATION

This work was supported, in part, by National Institutes of Health grants CA034196 (L.D. Shultz), AI132963 (M.A. Brehm, L.D. Shultz), OD026440 (D.L. Greiner, M.A. Brehm, L.D. Shultz), and NIDDK-supported Human Islet Research Network (HIRN, <https://hirnetwork.org>) DK104218. This work was funded, in part, by the UK Department of Health's Policy Research Programme, Grant Number 044/0069 (S. Vessillier). The views expressed in the publication are those of the author(s) and not necessarily those of the NHS, the NIHR, the Department of Health, 'arms' length bodies, or other government departments."

DISCLOSURES

The contents of this publication are solely the responsibility of the authors and do not necessarily represent the official views of the National Institutes of Health. M.A. Brehm and D.L. Greiner receive research support and are consultants for The Jackson Laboratory. The other authors declare no potential conflicts of interest.

DATA AVAILABILITY STATEMENT

The raw data supporting the conclusions of this article will be made available by the authors, without undue reservation.

ETHICS APPROVAL

Human PBMC recovered from leukopaks purchased from either Lonza (Basel, Switzerland) or StemCell Technologies (Vancouver, British Columbia). All animal procedures were done in accordance with the guidelines of the Animal Care and Use Committee of The Jackson Laboratory and The University of Massachusetts Medical School and conformed to the recommendations in the *Guide for the Care and Use of Laboratory Animals* (Institute of Laboratory Animal Resources, National Research Council, and National Academy of Sciences, 1996).

ORCID

Jiwon Yang  <https://orcid.org/0000-0003-4226-7224>

Michael A. Brehm  <https://orcid.org/0000-0001-6813-3262>

REFERENCES

1. Farkona S, Diamandis EP, Blasutig IM. Cancer immunotherapy: the beginning of the end of cancer? *BMC Med.* 2016;14:73.

2. Im A, Pavletic SZ. Immunotherapy in hematologic malignancies: past, present, and future. *J Hematol Oncol.* 2017;10:94.
3. Goebeler ME, Bargou RC. T cell-engaging therapies—BiTEs and beyond. *Nat Rev Clin Oncol.* 2020;17:418-434.
4. Jin S, Sun Y, Liang X, et al. Emerging new therapeutic antibody derivatives for cancer treatment. *Signal Transduct Target Ther.* 2022;7:39.
5. Slaney CY, von Scheidt B, Davenport AJ, et al. Dual-specific chimeric antigen receptor T cells and an indirect vaccine eradicate a variety of large solid tumors in an immunocompetent, self-antigen setting. *Clin Cancer Res.* 2017;23:2478-2490.
6. Philip M, Schietinger A. CD8(+) T cell differentiation and dysfunction in cancer. *Nat Rev Immunol.* 2021;22:209-223.
7. Waldman AD, Fritz JM, Lenardo MJ. A guide to cancer immunotherapy: from T cell basic science to clinical practice. *Nat Rev Immunol.* 2020;20:651-668.
8. Brinkmann U, Kontermann RE. The making of bispecific antibodies. *MAbs.* 2017;9:182-212.
9. Dreier T, Baeuerle PA, Fichtner I, et al. T cell costimulus-independent and very efficacious inhibition of tumor growth in mice bearing subcutaneous or leukemic human B cell lymphoma xenografts by a CD19-/CD3- bispecific single-chain antibody construct. *J Immunol.* 2003;170:4397-4402.
10. Spiess C, Zhai Q, Carter PJ. Alternative molecular formats and therapeutic applications for bispecific antibodies. *Mol Immunol.* 2015;67:95-106.
11. Staerz UD, Kanagawa O, Bevan MJ. Hybrid antibodies can target sites for attack by T cells. *Nature.* 1985;314:628-631.
12. Labrijn AF, Janmaat ML, Reichert JM, Parren PW. Bispecific antibodies: a mechanistic review of the pipeline. *Nat Rev Drug Discovery.* 2019;18:585-608.
13. Stein A, Franklin JL, Chia VM, et al. Benefit-risk assessment of blinatumomab in the treatment of relapsed/refractory B-cell precursor acute lymphoblastic leukemia. *Drug Saf.* 2019;42:587-601.
14. Zhao J, Song Y, Liu D. Recent advances on blinatumomab for acute lymphoblastic leukemia. *Exp Hematol Oncol.* 2019;8:28.
15. Goebeler ME, Bargou R. Blinatumomab: a CD19/CD3 bispecific T cell engager (BiTE) with unique anti-tumor efficacy. *Leuk Lymphoma.* 2016;57:1021-1032.
16. Gokbuget N, Dombret H, Bonifacio M, et al. Blinatumomab for minimal residual disease in adults with B-cell precursor acute lymphoblastic leukemia. *Blood.* 2018;131:1522-1531.
17. Kantarjian H, Stein A, Gokbuget N, et al. Blinatumomab versus chemotherapy for advanced acute lymphoblastic leukemia. *N Engl J Med.* 2017;376:836-847.
18. Topp MS, Gokbuget N, Zugmaier G, et al. Phase II trial of the anti-CD19 bispecific T cell-engager blinatumomab shows hematologic and molecular remissions in patients with relapsed or refractory B-precursor acute lymphoblastic leukemia. *J Clin Oncol.* 2014;32:4134-4140.
19. Zugmaier G, Gokbuget N, Klinger M, et al. Long-term survival and T-cell kinetics in relapsed/refractory ALL patients who achieved MRD response after blinatumomab treatment. *Blood.* 2015;126:2578-2584.
20. Morris EC, Neelapu SS, Giavridis T, Sadelain M. Cytokine release syndrome and associated neurotoxicity in cancer immunotherapy. *Nat Rev Immunol.* 2021;22:85-96.
21. Maude SL, Barrett D, Teachey DT, Grupp SA. Managing cytokine release syndrome associated with novel T cell-engaging therapies. *Cancer J.* 2014;20:119-122.
22. Liu D, Zhao J. Cytokine release syndrome: grading, modeling, and new therapy. *J Hematol Oncol.* 2018;11:121.
23. Shimabukuro-Vornhagen A, Godel P, Subklewe M, et al. Cytokine release syndrome. *J Immunother Cancer.* 2018;6:56.
24. Vessillier S, Eastwood D, Fox B, et al. Cytokine release assays for the prediction of therapeutic mAb safety in first-in-man trials—whole blood cytokine release assays are poorly predictive for TGN1412 cytokine storm. *J Immunol Methods.* 2015;424:43-52.
25. Finco D, Grimaldi C, Fort M, et al. Cytokine release assays: current practices and future directions. *Cytokine.* 2014;66:143-155.
26. Vessillier S, Fort M, O'Donnell L, et al. Development of the first reference antibody panel for qualification and validation of cytokine release assay platforms—report of an international collaborative study. *Cytokine X.* 2020;2:100042.
27. Frey N. Cytokine release syndrome: who is at risk and how to treat. *Best Pract Res Clin Haematol.* 2017;30:336-340.
28. Bareham B, Georgakopoulos N, Matas-Cespedes A, Curran M, Saeb-Parsy K. Modeling human tumor-immune environments in vivo for the preclinical assessment of immunotherapies. *Cancer Immunol, Immunother.* 2021;70:2737-2750.
29. Mestas J, Hughes CC. Of mice and not men: differences between mouse and human immunology. *J Immunol.* 2004;172:2731-2738.
30. Bryant CE, Monie TP. Mice, men and the relatives: cross-species studies underpin innate immunity. *Open Biol.* 2012;2:120015.
31. Ye C, Yang H, Cheng M, et al. A rapid, sensitive, and reproducible in vivo PBMC humanized murine model for determining therapeutic-related cytokine release syndrome. *FASEB J.* 2020;34:12963-12975.
32. Matas-Cespedes A, Brown L, Mahubani KT, et al. Use of human splenocytes in an innovative humanised mouse model for prediction of immunotherapy-induced cytokine release syndrome. *Clin Transl Immunol.* 2020;9:e1202.
33. Weaver JL, Zadrozny LM, Gabrielson K, Semple KM, Shea KI, Howard KE. BLT-immune humanized mice as a model for nivolumab-induced immune-mediated adverse events: comparison of the NOG and NOG-EXL strains. *Toxicol Sci.* 2019;169:194-208.
34. Yan H, Bhagwat B, Sanden D, et al. Evaluation of a TGN1412 analogue using in vitro assays and two immune humanized mouse models. *Toxicol Appl Pharmacol.* 2019;372:57-69.
35. Strober W. Obtaining human peripheral blood cells. *Curr Protoc Immunol.* 1997;21:A.3F.1-A.3F.2.
36. Hijazi Y, Klinger M, Kratzer A, et al. Pharmacokinetic and pharmacodynamic relationship of blinatumomab in patients with non-Hodgkin lymphoma. *Curr Clin Pharmacol.* 2018;13:55-64.
37. Brehm MA, Kenney LL, Wiles MV, et al. Lack of acute xenogeneic graft-versus-host disease, but retention of T-cell function following engraftment of human peripheral blood mononuclear cells in NSG mice deficient in MHC class I and II expression. *FASEB J.* 2019;33:3137-3151.
38. Salles G, Barrett M, Foa R, et al. Rituximab in B-cell hematologic malignancies: a review of 20 years of clinical experience. *Adv Ther.* 2017;34:2232-2273.
39. Teachey DT, Rheingold SR, Maude SL, et al. Cytokine release syndrome after blinatumomab treatment related to abnormal macrophage activation and ameliorated with cytokine-directed therapy. *Blood.* 2013;121:5154-5157.

40. Einsele H, Borghaei H, Orlowski RZ, et al. The BiTE (bispecific T-cell engager) platform: development and future potential of a targeted immuno-oncology therapy across tumor types. *Cancer*. 2020;126:3192-3201.
41. Jen EY, Xu Q, Schetter A, et al. FDA approval: blinatumomab for patients with B-cell precursor acute lymphoblastic leukemia in morphologic remission with minimal residual disease. *Clin Cancer Res*. 2019;25:473-477.
42. Klinger M, Brandl C, Zugmaier G, et al. Immunopharmacologic response of patients with B-lineage acute lymphoblastic leukemia to continuous infusion of T cell-engaging CD19/CD3-bispecific BiTE antibody blinatumomab. *Blood*. 2012;119:6226-6233.
43. Zhu M, Wu B, Brandl C, et al. Blinatumomab, a bispecific T-cell engager (BiTE((R))) for CD-19 targeted cancer immunotherapy: clinical pharmacology and its implications. *Clin Pharmacokinet*. 2016;55:1271-1288.
44. Shen J, Swift B, Mamelok R, Pine S, Sinclair J, Attar M. Design and conduct considerations for first-in-human trials. *Clin Transl Sci*. 2019;12:6-19.
45. d'Argouges S, Wissing S, Brandl C, et al. Combination of rituximab with blinatumomab (MT103/MEDI-538), a T cell-engaging CD19-/CD3-bispecific antibody, for highly efficient lysis of human B lymphoma cells. *Leuk Res*. 2009;33:465-473.
46. Kulkarni HS, Kasi PM. Rituximab and cytokine release syndrome. *Case Rep Oncol*. 2012;5:134-141.
47. Li J, Piskol R, Ybarra R, et al. CD3 bispecific antibody-induced cytokine release is dispensable for cytotoxic T cell activity. *Sci Transl Med*. 2019;11:11.
48. Rogala B, Freyer CW, Ontiveros EP, Griffiths EA, Wang ES, Wetzler M. Blinatumomab: enlisting serial killer T-cells in the war against hematologic malignancies. *Expert Opin Biol Ther*. 2015;15:895-908.
49. Morcos PN, Li J, Hosseini I, Li CC. Quantitative clinical pharmacology of T-cell engaging Bispecifics: current perspectives and opportunities. *Clin Transl Sci*. 2021;14:75-85.
50. King MA, Covassin L, Brehm MA, et al. Human peripheral blood leucocyte non-obese diabetic-severe combined immunodeficiency interleukin-2 receptor gamma chain gene mouse model of xenogeneic graft-versus-host-like disease and the role of host major histocompatibility complex. *Clin Exp Immunol*. 2009;157:104-118.

SUPPORTING INFORMATION

Additional supporting information can be found online in the Supporting Information section at the end of this article.

How to cite this article: Yang J, Jiao J, Draheim KM, et al. Simultaneous evaluation of treatment efficacy and toxicity for bispecific T-cell engager therapeutics in a humanized mouse model. *The FASEB Journal*. 2023;37:e22995. doi:[10.1096/fj.202300040R](https://doi.org/10.1096/fj.202300040R)